RAA 2016 Vol. **16** No. **6**, 96 (8pp) doi: 10.1088/1674–4527/16/6/096
http://www.raa-journal.org *http://iopscience.iop.org/raa*

Research in Astronomy and Astrophysics

The high-amplitude δ Scuti variable CY Aqr is probably a triple system

Wei-Jing Fang[1], Zhi-Quan Luo[1], Xiao-Bin Zhang[2], Li-Cai Deng[2], Kun Wang[2], Yang-Ping Luo[1], Yang Pan[1], Yin-Jiang Peng[1]

[1] Physics and Space Science College, China West Normal University, Nanchong 637002, China; *nczqluo@126.com; fangwjap@163*

[2] Key Laboratory of Optical Astronomy, National Astronomical Observatories, Chinese Academy of Sciences, Beijing, 100012, China

Received 2015 December 29; accepted 2016 February 5

Abstract Data representing 864 times of light maxima of the high-amplitude δ Scuti star CY Aqr were collected from the literature, based on which, long-term period changes of the variable star were investigated. A revised period and new ephemerides were given for the pulsating star. Remarkable cyclic variations were found in the $O-C$ residuals which can be attributed to the light-time effects due to probable unseen components of the object. By using Kopal's method, the orbital parameters of the supposed component stars were derived. The solution suggests that CY Aqr is very probably in a triple system orbited eccentrically by two low-mass companions with periods of 54.2 and 47.3 yr. The lower limits on masses were estimated as 0.04 $M_\odot$ and 0.02 $M_\odot$, respectively, for the two hidden companions.

Key words: methods: data analysis — stars: variables: δ Scuti — stars: individual (CY Aqr)

1 INTRODUCTION

δ Scuti stars are in the core or shell hydrogen burning stage of evolution. On the Hertzsprung-Russell Diagram, they are located around the intersection of the classical instability strip and the main sequence. The masses of these stars range from 1.5 $M_\odot$ to 2.5 $M_\odot$, and they usually pulsate in multiple modes with periods between 18 min and 8 h, and amplitudes from mmag up to tenths of a magnitude (Yang et al. 2012). High-amplitude δ Scuti stars (HADS) are characterized by pulsation periods shorter than 0.25 days, pulsation amplitudes larger than 0.1 mag and a spectral type between A3 and F5 (Boonyarak et al. 2011). SX Phoenicis stars, a subgroup of HADS, are low-metallicity old Population II stars (Yang et al. 2012). Pulsation in δ Scuti stars allows the study of the internal structure and evolution. For this reason they have been extensively observed and studied. Recently, many investigations have revealed that some HADS are actually in binary systems and usually show long-term orbital period variations (Derekas et al. 2009). These changes are typically displayed in an $O-C$ plot, in which the differences between the observed times of light maxima and those predicted by the original ephemeris are displayed as a function of Julian Date. For a given period, the residuals are distributed along $O-C$ around 0. If the period applied is incorrect, the residuals are distributed somewhat aslant with a slope (Sterken 2005). Many HADS have an even more complex $O-C$ diagram in which the cause of their variations remains a mystery.

CY Aqr is a well studied SX Phoenicis star which was discovered in the 1930s (Jensch 1934). Because of its short period (88 min) and large amplitude (0.74 mag in V), CY Aqr has been extensively observed for more than eight decades. Hardie & Tolbert (1961) contributed the first photoelectric photometry of CY Aqr in the UBV system and noted the gradual decrease of its pulsation period. After that, the period changes of the star attracted considerable attention (Percy 1975, Mahdy & Szeidl 1980, Rolland et al. 1986, Coates et al. 1994). A number of interpretations were postulated to explain the discrepancies between the observed and calculated times of light maxima (Powell et al. 1995). Coates et al. (1994) suggested that the shape of the $O-C$ diagram might be due to a light-time effect in a binary system. Under such assumption, Fu & Sterken (2003) derived a reliable model for the period variation of CY Aqr. Their solution yielded a 52.5 yr highly eccentric orbit for the probable companion. The binary explanation, however, could not account for the full range of period changes. The mysterious period variation of CY Aqr is still not understood.

Pursuing an accurate determination of the period variation of CY Aqr, after Fu & Sterken (2003) was published, we carried out an extensive literature search and collected a large number of new times of light maxima. Based on the $O-C$ method, the long-term period behavior of CY Aqr was investigated.

2 OBSERVATIONAL DATA

As a result of an extensive literature survey of CY Aqr, we were able to find 864 times of light maxima between 1934 and 2015. These data are shown in Table 1.

Since the times of light maxima were obtained by different observation techniques as technology advanced, from visual, to photographic, photoelectric and CCD, the sensitivity and accuracy in the collection have a huge range. In order to combine such a diverse data set, we assign different weights to each method so that the issue of data quality can be reasonably taken into account. We use weight $=1$ for visual records, 4 for photographic data, and 10 for photoelectric and CCD measurements.

3 NEW LINEAR EPHEMERIS AND THE CYCLIC CHANGE IN THE $O-C$ DIAGRAM

Using all 864 times of light maxima in Table 1 and applying weights to the different data types, the best fitting gives the following new linear ephemeris.

$$\mathrm{Max.(HJD)} \;=\; 2453334.9426(\pm 0.0001) + 0.061038381(\pm 0.0000000006) \times E, \tag{1}$$

where E is the number of cycles. The $O-C$ curve computed with the ephemeris given in Equation (1) is displayed in Figure 1 (top panel), in which an obvious cyclic residual signal exists. Such an $O-C$ residual pattern is normally interpreted as the light-time effect in a binary system (Coates et al. 1994, Fu & Sterken 2003). According to the prescription of Fu & Sterken (2003), we assumed the existence of one companion star around CY Aqr. Therefore, the following method was used to analyze the $O-C$ data. First, the approximate frequency harmonics and amplitudes can be recognized by using the discrete Fourier transformation method. These frequencies are then refined with the following fitting

$$O-C(t) \;=\; 0.5a_0 + \sum_{k=1}^{2}\left[a_k \sin\left(\frac{2\pi k t}{P_1}\right) + b_k \cos\left(\frac{2\pi k t}{P_1}\right)\right]. \tag{2}$$

The results of the fitting are shown in Figure 1. The top panel gives the $O-C$ data and the solid line shows the fit derived by Equation (2). The bottom panel shows the residuals from subtracting the solid line of the top panel. The orbital parameters can then be computed from the Fourier coefficients (Kopal 1978) as follows

$$e' = 2\sqrt{\frac{{a_2}^2 + {b_2}^2}{{a_1}^2 + {b_1}^2}}, \tag{3}$$

where a_1, a_2, b_1 and b_2 are the Fourier coefficients, and e' is the eccentricity of the long-period orbit. Using the method above, we obtained the eccentricity for the long-period orbit, and we find that $e' > 1$. As shown in the lower panel of Figure 1, the fitting residual has a strong periodic signal after extracting the primary orbital period. Therefore, a single companion scenario cannot fully explain the $O-C$ diagram.

In order to validate our conjecture, we assume an additional star and re-fit a curve with the following form to the $O-C$ data

$$O-C(t) \;=\; 0.5a_0 + \sum_{k=1}^{2}\left[a_k \sin\left(\frac{2\pi k t}{P_1}\right) + b_k \cos\left(\frac{2\pi k t}{P_1}\right)\right] + \sum_{k=1}^{2}\left[c_k \sin\left(\frac{2\pi k t}{P_2}\right) + d_k \cos\left(\frac{2\pi k t}{P_2}\right)\right], \tag{4}$$

where the first Fourier transform term is for the first companion and the other is for the second star.

The fitting diagram is provided in Figure 2. The top panel shows the new $O-C$ data and the solid line shows the fit derived by Equation (4). The bottom panel shows the residuals from subtracting the solid line of the top panel, where no variation can be found.

4 RESULTS

Comparing Figures 1 and 2, and noting the final residual in the lower panel of Figure 2, it is clear that a triple system with two companions is more feasible for CY Aqr than previous studies. On the basis of the spectral type of δ Scuti stars (Chang et al. 2013), the mass of CY Aqr is estimated

Table 1 Times of Light Maxima of CY Aqr

$T_{\max}$	Detector	Ref	$T_{\max}$	Detector	Ref	$T_{\max}$	Detector	Ref	$T_{\max}$	Detector	Ref	$T_{\max}$	Detector	Ref
27013.2930	pg	[1]	36546.0949	pe	[1]	43011.5832	vis	[9]	47410.4283	pe	[1]	53569.5167	CCD	[19]
27413.2200	pg	[1]	36546.1555	pe	[1]	43011.6412	vis	[9]	47410.4891	pe	[1]	53605.7721	CCD	[13]
27659.5067	pg	[2]	36549.0860	pe	[1]	43012.4361	vis	[9]	47411.4047	pe	[1]	53612.3657	CCD	[19]
27668.9730	pg	[2]	36549.1472	pe	[1]	43012.4971	vis	[9]	47411.4661	pe	[1]	53612.4269	CCD	[19]
27671.5317	pg	[1]	36568.0690	pe	[1]	43012.5573	vis	[9]	47411.5265	pe	[1]	53612.4878	CCD	[19]
27671.5299	pg	[1]	36569.0457	pe	[1]	43012.6185	vis	[9]	47411.5871	pe	[1]	53612.5483	CCD	[19]
27682.5211	pg	[1]	36569.1069	pe	[1]	43014.5121	vis	[9]	47792.7727	pe	[1]	53613.7080	CCD	[13]
27684.9629	pg	[1]	36570.0834	pe	[1]	43014.5732	vis	[9]	47792.8338	pe	[1]	53613.7678	CCD	[13]
27688.9906	pg	[1]	36735.8044	pe	[1]	43014.6326	vis	[9]	47792.8948	pe	[1]	53647.0339	CCD	[13]
27690.3940	pg	[1]	36735.8654	pe	[1]	43015.4880	vis	[9]	47799.6702	pe	[1]	53682.3752	CCD	[13]
27692.5287	pg	[1]	36740.9929	pe	[2]	43016.4644	vis	[9]	47799.7313	pe	[1]	53683.2906	CCD	[13]
27692.6520	pg	[1]	36749.7819	pe	[1]	43016.5256	vis	[9]	47799.7924	pe	[1]	53683.3517	CCD	[13]
27693.3829	pg	[1]	36749.8432	pe	[1]	43016.5906	vis	[9]	47799.8534	pe	[1]	53684.3285	CCD	[13]
27693.4462	pg	[1]	36792.6920	pe	[1]	43017.3802	vis	[9]	47801.6844	pe	[1]	53688.3568	CCD	[13]
27694.3590	pg	[1]	36792.7528	pe	[1]	43017.4416	vis	[9]	47801.7456	pe	[1]	53689.3337	CCD	[13]
27695.4600	pg	[1]	36792.8750	pe	[1]	43017.5012	vis	[9]	47801.8064	pe	[1]	53989.3372	CCD	[13]
27696.6793	pg	[1]	36792.9367	pe	[2]	43017.5618	vis	[9]	47807.6051	pe	[1]	53989.3980	CCD	[13]
27697.4721	pg	[1]	36803.8012	pe	[1]	43017.6243	vis	[9]	47807.6664	pe	[1]	54007.0997	CCD	[13]
27702.0519	pg	[1]	36803.8617	pe	[1]	43018.3583	vis	[9]	47807.7273	pe	[1]	54008.7473	CCD	[13]
27710.5949	pg	[1]	36832.6114	pe	[1]	43018.4184	vis	[9]	47807.7882	pe	[1]	54032.4907	CCD	[13]
27712.3069	pg	[1]	36832.7330	pe	[1]	43018.4788	vis	[9]	47807.8494	pe	[1]	54032.5523	CCD	[13]
27717.4332	pg	[1]	36835.6017	pe	[1]	43018.5420	vis	[9]	47818.7141	pe	[1]	54092.2510	CCD	[13]
27744.2302	pg	[1]	36835.6624	pe	[1]	43018.6004	vis	[9]	47818.7752	pe	[1]	54092.3110	CCD	[13]
27744.2909	pg	[1]	36838.7150	pe	[2]	43401.3706	pe	[1]	48022.0354	pe	[3]	54307.5293	CCD	[13]
28035.3842	pg	[1]	36842.6818	pe	[1]	43401.4327	pe	[1]	48065.9203	pe	[1]	54308.5073	CCD	[13]
28045.3924	pg	[1]	36842.7430	pe	[1]	43401.4937	pe	[1]	48070.9257	pe	[1]	54381.4464	CCD	[20]
28046.3071	pg	[1]	36845.7345	pe	[1]	43402.3478	pe	[1]	48099.7970	pe	[1]	54410.5627	CCD	[13]
28046.4901	pg	[1]	36871.1246	pe	[1]	43402.4086	pe	[1]	48530.6693	pe	[1]	54671.5630	CCD	[13]
28047.2826	pg	[1]	36902.0108	pe	[1]	43402.4699	pe	[1]	48530.7302	pe	[1]	54709.4677	CCD	[13]
28047.3464	pg	[1]	36902.0716	pe	[1]	43402.5311	pe	[1]	48531.6459	pe	[1]	54729.3056	CCD	[13]
28047.4064	pg	[1]	36903.0490	pe	[1]	43425.4207	pe	[1]	48531.7068	pe	[1]	54729.3665	CCD	[13]
28047.4668	pg	[1]	36906.0397	pe	[1]	43425.4814	pe	[1]	48531.7679	pe	[1]	54729.4272	CCD	[13]
28048.3823	pg	[1]	36928.0728	pe	[1]	43482.2454	pe	[1]	48813.8885	pe	[1]	54730.2815	CCD	[13]
28074.3254	pg	[1]	36928.1343	pe	[1]	43490.2434	pe	[1]	48887.7451	pe	[1]	54730.3428	CCD	[13]
28074.3860	pg	[1]	36928.9895	pe	[1]	43490.3038	pe	[1]	48888.9048	pe	[1]	54730.4039	CCD	[13]
28090.3189	pg	[1]	36929.0511	pe	[1]	43815.3325	pe	[1]	49199.8356	pe	[1]	54730.4647	CCD	[13]
28090.3800	pg	[1]	36929.1105	pe	[1]	43815.3636	pe	[5]	49199.8964	pe	[1]	54734.3710	CCD	[13]
28092.1508	pg	[1]	37195.7276	pe	[1]	43815.3947	pe	[1]	49199.9578	pe	[1]	54734.4318	CCD	[13]
28094.2860	pg	[1]	37195.7894	pe	[1]	44158.3069	pe	[1]	49222.8470	pe	[1]	54736.3854	CCD	[13]
28397.5233	pg	[1]	37196.6432	pe	[1]	44896.6878	pe	[1]	49275.6441	CCD	[1]	54738.3388	CCD	[13]
28422.4259	pg	[1]	37198.2906	pe	[1]	45194.7999	pe	[1]	49280.0396	pe	[3]	54738.3993	CCD	[13]
28422.4874	pg	[1]	37202.1968	pe	[1]	45194.8583	pe	[1]	49281.0776	pe	[3]	54738.3999	CCD	[13]
28422.5490	pg	[1]	37204.1506	pe	[1]	45194.9208	pe	[1]	49281.1390	pe	[3]	54739.3754	CCD	[13]
28423.3418	pg	[1]	37222.1557	pe	[1]	45195.7756	pe	[1]	49282.0540	pe	[3]	54749.3254	CCD	[13]
28423.4027	pg	[1]	37222.2165	pe	[1]	45195.8979	pe	[1]	49282.1150	pe	[3]	54749.3867	CCD	[13]
28423.4650	pg	[1]	37224.2303	pe	[1]	45199.8034	pe	[1]	49282.1760	pe	[3]	54757.2605	CCD	[13]
28423.5251	pg	[1]	37225.6365	pe	[1]	45199.9249	pe	[1]	49283.0313	pe	[3]	54757.3214	CCD	[13]
28434.6347	pg	[1]	37225.6978	pe	[1]	45199.9868	pe	[1]	49283.0915	pe	[3]	54757.3825	CCD	[13]
28445.8052	pg	[1]	37226.1231	pe	[1]	45207.4944	pe	[1]	49286.6322	CCD	[1]	54761.2892	CCD	[13]
28451.4802	pg	[1]	37233.6340	pe	[1]	45543.6319	pe	[1]	49290.7218	pe	[1]	54761.3503	CCD	[13]
28501.2275	pg	[1]	37233.6940	pe	[1]	45544.6092	pe	[1]	49328.9938	pe	[3]	54781.2485	CCD	[13]
28501.2878	pg	[1]	37250.1112	pe	[1]	45544.6698	pe	[1]	49567.8366	CCD	[1]	54781.3091	CCD	[13]
28623.3071	pg	[1]	37253.1013	pe	[1]	45584.7726	pe	[1]	49623.6258	CCD	[1]	54796.2637	CCD	[13]

Notes: $T_{\max}$ is in HJD–2400000. The references (column "Ref") are the following: [1] Powell et al. (1995); [2] Percy (1975); [3] Fu & Sterken (2003); [4] Ashbrook (1949); [5] Rolland et al. (1986); [6] Smak (1959); [7] Braune et al. (1977); [8] Braune et al. (1979); [9] Figer (1978); [10] Agerer & Hubscher (1996); [11] Agerer & Huebscher (1998a); [12] Agerer & Huebscher (1998b); [13] Tuvikene et al. (2010); [14] Agerer et al. (1999); [15] Agerer et al. (2001); [16] Agerer & Hubscher (2002); [17] Agerer & Hubscher (2003); [18] Hubscher et al. (2012); [19] Hubscher et al. (2009a); [20] Hubscher et al. (2009b); [21] Hubscher & Monninger (2011); [22] Wils et al. (2011); [23] Hubscher (2011); [24] Sterken et al. (2011); [25] Paschke (2010); [26] Hubscher & Lehmann (2012); [27] Sterken et al. (2012); [28] Wils et al. (2012); [29] Wils et al. (2013); [30] Wils et al. (2014); [31] Samolyk (2014); [32] Samolyk (2015).

Table 1 — *Continued*

$T_{\max}$	Detector	Ref	$T_{\max}$	Detector	Ref	$T_{\max}$	Detector	Ref	$T_{\max}$	Detector	Ref	$T_{\max}$	Detector	Ref
28782.5534	pg	[1]	37255.1161	pe	[1]	45587.7023	pe	[1]	49623.6869	CCD	[1]	54796.3253	CCD	[13]
28865.2605	pg	[2]	37257.1307	pe	[1]	45587.7636	pe	[1]	49623.7481	CCD	[1]	54809.2041	CCD	[13]
29079.8141	vis	[3]	37524.5425	pe	[1]	45587.8243	pe	[1]	49625.6401	CCD	[1]	54809.2648	CCD	[13]
29085.7353	vis	[3]	37578.1311	pe	[1]	45588.7399	pe	[1]	49625.7012	CCD	[1]	54827.2105	CCD	[13]
29085.7950	vis	[3]	37578.1930	pe	[1]	45588.8010	pe	[1]	49625.7623	CCD	[1]	55063.4284	CCD	[21]
29085.8545	vis	[3]	37578.2539	pe	[1]	45588.8621	pe	[1]	50027.2749	CCD	[10]	55063.4918	CCD	[21]
29086.7710	vis	[3]	37583.1360	pe	[1]	45589.7167	pe	[1]	50027.3360	CCD	[10]	55085.4631	CCD	[13]
29086.8314	vis	[3]	37583.1980	pe	[1]	45589.7779	pe	[1]	50072.9916	CCD	[3]	55085.4633	CCD	[13]
29088.7853	vis	[3]	38643.4958	pe	[1]	45589.8386	pe	[1]	50401.0125	CCD	[3]	55085.4641	CCD	[13]
29107.7670	vis	[3]	38644.4117	pe	[1]	45590.6934	pe	[1]	50401.0735	CCD	[3]	55114.3956	CCD	[13]
29108.7415	vis	[3]	38645.3895	pe	[1]	45590.7543	pe	[1]	50401.1345	CCD	[3]	55114.3957	CCD	[13]
29195.3568	pg	[1]	38645.4508	pe	[1]	45590.8154	pe	[1]	50401.9888	CCD	[3]	55114.3964	CCD	[13]
29198.1654	pg	[2]	38652.4082	pe	[1]	45590.8766	pe	[1]	50439.2230	CCD	[11]	55157.2436	CCD	[13]
29201.3382	pg	[1]	38652.4693	pe	[1]	45592.7076	pe	[1]	50683.4980	pe	[12]	55157.2449	CCD	[13]
29568.3020	pg	[1]	38653.4454	pe	[1]	45592.7682	pe	[3]	50683.5610	pe	[12]	55157.2452	CCD	[13]
29578.8016	pg	[1]	38654.4835	pe	[1]	45592.8294	pe	[1]	50683.6210	pe	[12]	55434.3598	CCD	[22]
29589.2989	pg	[1]	38660.0051	pe	[5]	45611.3853	pe	[1]	50720.4871	CCD	[12]	55434.4205	CCD	[22]
29880.4529	pg	[1]	38675.2981	pe	[1]	45611.4465	pe	[1]	50749.2362	CCD	[12]	55434.4816	CCD	[22]
29904.8686	pg	[2]	38675.3592	pe	[1]	45612.3625	pe	[1]	50749.2974	CCD	[12]	55446.3830	CCD	[23]
31268.8978	pg	[1]	38676.3344	pe	[1]	45612.4244	pe	[1]	50749.3581	CCD	[12]	55460.3611	CCD	[24]
31291.6650	pg	[2]	38680.7300	pe	[1]	45612.6671	pe	[1]	51107.6543	CCD	[13]	55460.4222	CCD	[24]
31296.9139	pg	[1]	38680.7910	pe	[1]	45612.7268	pe	[1]	51115.5893	CCD	[13]	55469.3340	CCD	[24]
31297.8304	pg	[1]	38970.9063	pe	[1]	45612.7883	pe	[1]	51115.6503	CCD	[13]	55469.3948	CCD	[24]
31742.4357	vis	[2]	38978.9024	pe	[1]	45616.6963	pe	[1]	51162.6502	CCD	[13]	55481.2973	CCD	[24]
31750.4951	vis	[3]	38997.8219	pe	[1]	45616.7563	pe	[1]	51129.2612	CCD	[14]	55481.3584	CCD	[22]
31751.4676	vis	[3]	38997.9459	pe	[1]	45616.8174	pe	[1]	51129.3222	CCD	[14]	55484.2878	CCD	[24]
31751.4716	vis	[3]	39003.8678	pe	[1]	45621.3351	pe	[1]	51420.3560	pe	[15]	55484.3493	CCD	[24]
31751.5291	vis	[3]	39003.9282	pe	[1]	45629.3301	pe	[1]	51432.5627	CCD	[3]	55484.4102	CCD	[24]
31751.5302	vis	[3]	39089.5647	pe	[1]	45631.2843	pe	[1]	51461.4940	CCD	[3]	55490.3309	CCD	[24]
31758.3651	vis	[2]	39350.6861	pe	[1]	45631.3453	pe	[1]	51462.4095	CCD	[3]	55496.3128	CCD	[24]
31758.3671	vis	[3]	39350.7490	pe	[1]	45633.6641	pe	[1]	51463.3864	CCD	[3]	55496.3744	CCD	[24]
31759.5265	vis	[2]	39350.8087	pe	[1]	45633.7248	pe	[1]	51463.4468	CCD	[3]	55498.2662	CCD	[24]
31765.5099	vis	[3]	39350.8692	pe	[1]	45634.6408	pe	[1]	51463.5085	CCD	[3]	55498.3270	CCD	[24]
31765.5107	vis	[3]	39351.7253	pe	[1]	45634.7018	pe	[1]	51483.3450	CCD	[15]	55498.3883	CCD	[24]
31765.5694	vis	[3]	39351.8460	pe	[1]	45634.7629	pe	[1]	51518.3830	pe	[15]	55505.2860	CCD	[25]
32091.3914	pg	[1]	39355.6920	pe	[1]	45635.3122	pe	[1]	51747.5215	pe	[16]	55505.3470	CCD	[25]
32091.4532	pg	[1]	39355.7546	pe	[1]	45635.3732	pe	[1]	51806.7891	CCD	[13]	55506.2618	CCD	[24]
32092.3061	pg	[2]	39355.8145	pe	[1]	45641.2940	pe	1	51806.7892	CCD	[13]	55506.3225	CCD	[24]
32092.3697	vis	[2]	39355.8763	pe	[1]	45641.3550	pe	[1]	51855.3760	CCD	[16]	55506.3837	CCD	[24]
32093.4056	pg	[1]	39356.7300	pe	[1]	45645.2621	pe	[1]	51873.3230	CCD	[16]	55530.2500	CCD	[24]
32422.7694	vis	[4]	39356.7908	pe	[1]	45645.3225	pe	[1]	51873.3830	CCD	[16]	55535.2553	CCD	[24]
32422.8321	vis	[4]	39356.8527	pe	[1]	45651.3634	pe	[1]	51887.2366	CCD	[16]	55535.3163	CCD	[24]
32436.6237	vis	[4]	39374.6443	pe	[5]	45661.2532	pe	[1]	52199.4480	CCD	[16]	55544.2280	CCD	[24]
32436.6839	vis	[4]	39384.6848	pe	[1]	45662.2920	pe	[1]	52253.2842	CCD	[16]	55547.2188	CCD	[24]
32438.7003	vis	[4]	39384.7455	pe	[1]	45904.2456	pe	[3]	52534.6710	CCD	[3]	55547.2800	CCD	[24]
32440.4700	pg	[1]	39384.8072	pe	[1]	45942.7622	pe	[1]	52535.7086	CCD	[3]	55793.4464	CCD	[26]
32443.5838	vis	[4]	39384.8675	pe	[1]	45942.8232	pe	[1]	52538.6990	CCD	[3]	55793.5077	CCD	[26]
32443.7033	vis	[4]	39384.9279	pe	[1]	45942.8843	pe	[1]	52538.7600	CCD	[3]	55793.5685	CCD	[26]
32445.7198	vis	[2]	39385.7240	pe	[1]	45942.9453	pe	[1]	52539.5534	CCD	[3]	55800.2847	CCD	[27]
32445.7817	vis	[4]	39385.7823	pe	[1]	45972.1828	pe	[3]	52539.6152	CCD	[3]	55800.3452	CCD	[27]
32464.5182	vis	[4]	39385.8448	pe	[1]	46055.5612	pe	[1]	52539.6753	CCD	[3]	55800.4066	CCD	[27]
32464.5804	vis	[4]	39385.9057	pe	[1]	46062.5806	pe	[1]	52539.7366	CCD	[3]	55800.4667	CCD	[27]
32465.5582	vis	[4]	39401.5920	pe	[1]	46063.5571	pe	[1]	52540.6521	CCD	[3]	55801.2607	CCD	[27]
32465.6168	vis	[4]	39401.6527	pe	[1]	46270.5393	pe	[1]	52540.7134	CCD	[3]	55801.3220	CCD	[27]
33099.8081	vis	[3]	39401.7139	pe	[1]	46271.4541	pe	[1]	52540.7752	CCD	[3]	55801.3828	CCD	[27]
33171.6528	vis	[3]	39405.6204	pe	[1]	46271.5154	pe	[1]	52541.5683	CCD	[3]	55801.4439	CCD	[27]
33171.7111	vis	[3]	39405.6822	pe	[1]	46297.3960	pe	[1]	52541.6293	CCD	[3]	55801.5050	CCD	[27]
33171.7737	vis	[3]	39405.7428	pe	[1]	46298.3726	pe	[1]	52541.6900	CCD	[3]	55826.3469	CCD	[27]
33172.7509	vis	[2]	39406.5980	pe	[1]	46298.4335	pe	[1]	52541.7514	CCD	[3]	55826.4079	CCD	[27]
33179.5285	vis	[3]	39406.6578	pe	[1]	46298.4949	pe	[1]	52557.4373	CCD	[17]	55831.3520	CCD	[27]

Table 1 — *Continued*

$T_{\max}$	Detector	Ref	$T_{\max}$	Detector	Ref	$T_{\max}$	Detector	Ref	$T_{\max}$	Detector	Ref	$T_{\max}$	Detector	Ref
33180.3789	vis	[2]	39406.7196	pe	[1]	46298.5557	pe	[1]	52625.5569	CCD	[3]	55831.4132	CCD	[27]
33180.6860	vis	[3]	40779.7783	pe	[1]	46648.4872	pe	[1]	52626.5339	CCD	[3]	55833.3662	CCD	[28]
33183.5557	vis	[3]	40779.8390	pe	[1]	46648.5479	pe	[1]	52821.9182	CCD	[13]	55838.3103	CCD	[27]
33183.6161	vis	[3]	40779.9005	pe	[1]	46648.6095	pe	[1]	52903.4032	CCD	[13]	55838.3718	CCD	[27]
33185.5702	vis	[3]	40892.6364	pe	[1]	46649.4631	pe	[1]	52920.9223	CCD	[13]	55848.3207	CCD	[28]
33560.4638	pe	[1]	40894.6507	pe	[1]	46649.5242	pe	[1]	52920.9827	CCD	[13]	55849.2971	CCD	[27]
33563.2728	pe	[1]	41126.5960	pe	[1]	46649.5856	pe	[1]	52921.0439	CCD	[13]	55849.3585	CCD	[27]
33563.3350	pe	[1]	41623.2647	pe	[1]	46650.5617	pe	[1]	52923.0587	CCD	[13]	55853.3258	CCD	[27]
33563.3947	pe	[1]	41958.3639	pe	[1]	46650.6231	pe	[1]	52926.9643	CCD	[13]	55853.3867	CCD	[27]
33860.5310	pg	[1]	41959.2799	pe	[1]	46651.4176	pe	[1]	52927.0258	CCD	[13]	55865.3505	CCD	[27]
33861.5070	pg	[1]	41959.3405	pe	[1]	46652.5156	pe	[1]	52930.3215	CCD	[13]	55865.4115	CCD	[27]
33861.5679	pg	[1]	41959.4018	pe	[1]	46652.5765	pe	[1]	52931.2981	CCD	[13]	55868.2802	CCD	[27]
33872.5565	pg	[1]	41959.4634	pe	[1]	46652.6375	pe	[1]	52931.3595	CCD	[13]	55868.3414	CCD	[27]
34253.5575	pg	[1]	41959.5234	pe	[1]	46659.7789	pe	[1]	53249.5522	CCD	[13]	55875.2385	CCD	[27]
34270.3440	pg	[1]	42257.5150	pe	[7]	46659.8406	pe	[1]	53250.5287	CCD	[13]	55875.2999	CCD	[27]
34282.7946	pe	[1]	42270.7584	pe	[1]	46659.9627	pe	[1]	53254.9840	CCD	[13]	55878.2906	CCD	[26]
34283.5887	pe	[1]	42270.8199	pe	[1]	47011.7872	pe	[1]	53256.3278	CCD	[13]	55879.3887	CCD	[26]
34283.6496	pe	[1]	42302.5015	pe	[1]	47011.8482	pe	[1]	53256.3883	CCD	[13]	55882.2581	CCD	[27]
34283.7102	pe	[1]	42302.5607	pe	[1]	47011.9092	pe	[1]	53256.8758	CCD	[13]	55882.3189	CCD	[27]
34283.7716	pe	[1]	42303.4778	pe	[1]	47025.8872	pe	[1]	53256.9374	CCD	[13]	55886.3477	CCD	[26]
34300.5572	pe	[1]	42303.5371	pe	[1]	47034.8596	pe	[1]	53286.4191	CCD	[13]	55886.5307	CCD	[27]
34300.6180	pe	[1]	42304.3927	pe	[1]	47037.7284	pe	[1]	53289.2884	CCD	[13]	55886.5916	CCD	[27]
34300.6792	pe	[1]	42304.4533	pe	[1]	47037.7892	pe	[1]	53289.4099	CCD	[13]	55887.2642	CCD	[26]
34307.6373	pe	[1]	42304.5126	pe	[1]	47037.8504	pe	[1]	53290.2660	CCD	[18]	55887.3242	CCD	[26]
34307.6983	pe	[1]	42313.3640	pe	[7]	47390.1634	pe	[1]	53290.3260	CCD	[18]	55887.5682	CCD	[27]
34308.4310	pe	[5]	42313.4250	pe	[7]	47390.2246	pe	[1]	53292.4012	CCD	[13]	55889.2167	CCD	[27]
34309.5295	pe	[1]	42325.3910	pe	[7]	47391.0177	pe	[1]	53304.3034	CCD	[13]	55889.2774	CCD	[27]
34309.5905	pe	[1]	42627.8323	pe	[1]	47392.7890	pe	[1]	53304.3649	CCD	[13]	55889.3388	CCD	[27]
34310.5065	pe	[1]	42627.8938	pe	[1]	47392.8487	pe	[1]	53306.3184	CCD	[13]	55889.5828	CCD	[27]
34310.5671	pe	[1]	42628.8093	pe	[1]	47392.9099	pe	[1]	53307.2334	CCD	[13]	55893.2453	CCD	[26]
34325.5219	pe	[1]	42628.8706	pe	[1]	47393.0932	pe	[1]	53307.2936	CCD	[13]	55893.3065	CCD	[26]
34325.5830	pe	[1]	42629.7855	pe	[1]	47393.1543	pe	[1]	53307.3556	CCD	[13]	55894.2222	CCD	[26]
34325.6435	pe	[1]	42629.8473	pe	[1]	47393.2155	pe	[1]	53307.4163	CCD	[13]	55894.2829	CCD	[26]
34354.4544	pe	[1]	42629.9076	pe	[1]	47393.8255	pe	[1]	53309.3698	CCD	[13]	55895.1984	CCD	[26]
34354.5149	pe	[1]	42654.6894	pe	[1]	47393.8867	pe	[1]	53311.3842	CCD	[13]	55895.2593	CCD	[26]
35032.4075	pe	[1]	42654.7498	pe	[1]	47394.1306	pe	[1]	53334.9453	CCD	[13]	55895.3202	CCD	[26]
35036.3750	pe	[1]	42654.8120	pe	[1]	47394.1917	pe	[1]	53336.9592	CCD	[13]	55896.2362	CCD	[26]
35036.4353	pe	[1]	42654.8722	pe	[1]	47395.7181	pe	[1]	53337.9357	CCD	[13]	55905.2695	CCD	[28]
35075.6218	pe	[1]	42658.7175	pe	[1]	47395.9011	pe	[1]	53556.8802	CCD	[13]	55915.2189	CCD	[27]
35361.4653	vis	[6]	42658.7784	pe	[1]	47395.9619	pe	[1]	53556.9409	CCD	[13]	55915.2800	CCD	[27]
35361.5278	vis	[6]	42658.8398	pe	[1]	47396.6947	pe	[1]	53557.7959	CCD	[13]	55923.2146	CCD	[27]
35366.4087	vis	[6]	42658.9005	pe	[1]	47396.7553	pe	[1]	53557.8567	CCD	[13]	55923.2760	CCD	[27]
35366.4701	vis	[6]	42660.8539	pe	[1]	47396.8163	pe	[1]	53557.9178	CCD	[13]	56134.4084	CCD	[29]
35367.3256	vis	[6]	42775.2430	pe	[8]	47396.8777	pe	[1]	53558.7723	CCD	[13]	56134.4694	CCD	[29]
35367.3847	vis	[6]	43008.4110	vis	[9]	47396.9387	pe	[1]	53558.8336	CCD	[13]	56168.5285	CCD	[29]
35367.5072	vis	[6]	43008.5308	vis	[9]	47398.0373	pe	[1]	53558.8945	CCD	[13]	56168.5896	CCD	[29]
35370.3752	vis	[6]	43008.5915	vis	[9]	47398.0984	pe	[1]	53559.7489	CCD	[13]	56233.3507	CCD	[29]
35370.4361	vis	[6]	43009.3870	vis	[9]	47398.1592	pe	[1]	53559.8101	CCD	[13]	56559.4172	CCD	[30]
35370.4992	vis	[6]	43009.4461	vis	[9]	47399.1358	pe	[1]	53559.8709	CCD	[13]	56579.5609	CCD	[31]
35370.5597	vis	[6]	43009.5065	vis	[9]	47399.1970	pe	[1]	53559.9320	CCD	[13]	56579.6214	CCD	[31]
35689.9121	pe	[1]	43009.5679	vis	[9]	47399.7463	pe	[1]	53561.7632	CCD	[13]	56579.6830	CCD	[31]
36487.1936	pe	[1]	43009.6309	vis	[9]	47399.8080	pe	[1]	53561.8244	CCD	[13]	56579.7441	CCD	[31]
36490.1231	pe	[1]	43010.3616	vis	[9]	47407.3763	pe	[1]	53563.7774	CCD	[13]	56579.8045	CCD	[31]
36490.1837	pe	[1]	43010.4233	vis	[9]	47407.4985	pe	[1]	53563.8387	CCD	[13]	56593.5391	CCD	[31]
36490.3068	pe	[1]	43010.4838	vis	[9]	47407.5588	pe	[1]	53563.8997	CCD	[13]	56593.5997	CCD	[31]
36491.2216	pe	[1]	43010.5440	vis	[9]	47408.3530	pe	[1]	53565.7310	CCD	[13]	56593.6605	CCD	[31]
36491.2831	pe	[1]	43010.6047	vis	[9]	47408.4140	pe	[1]	53565.7919	CCD	[13]	56603.6092	CCD	[31]
36492.1979	pe	[1]	43011.3971	vis	[9]	47408.5365	pe	[1]	53565.8526	CCD	[13]	56603.6708	CCD	[31]
36492.2595	pe	[1]	43011.4578	vis	[9]	47409.6962	pe	[1]	53565.9138	CCD	[13]	56930.4705	CCD	[32]
36492.3201	pe	[1]	43011.5208	vis	[9]	47409.7573	pe	[1]	53566.5233	CCD	[13]			

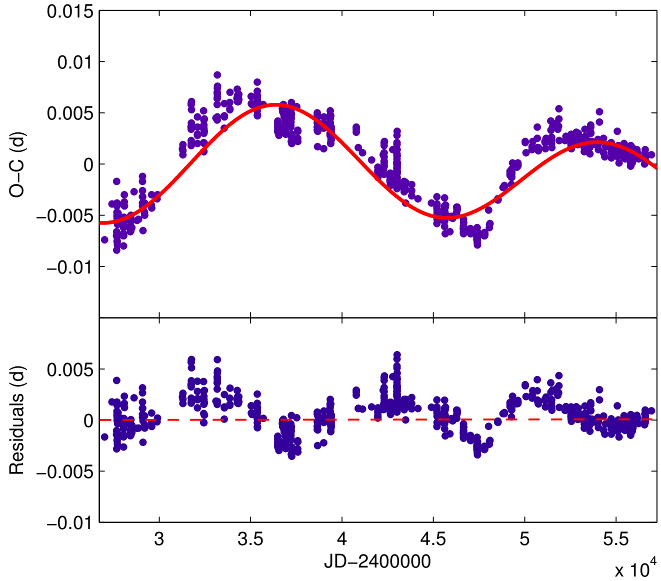

Fig. 1 The $O - C$ diagram (*top*) computed with the ephemeris given in Equation (1). The bottom panel shows the residuals obtained by subtracting Equation (2) (*top, solid line*).

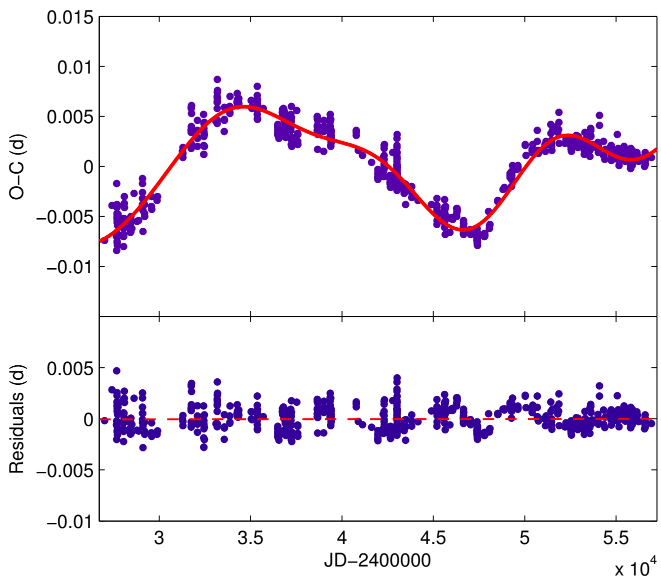

Fig. 2 The $O - C$ diagram (*top*) computed with the ephemeris given in Equation (1). The bottom panel shows the residuals obtained by subtracting Equation (4) (*top, solid line*).

as $M = 2.0\ M_\odot$. For the first companion star, the mass function can be derived based on the following formula

$$\begin{aligned} f(m_1) &= 4\pi^2(a_1' \sin i_1)^3/\mathrm{G}{P_1}^2 \\ &= (m_1 \sin i_1)^3/(M+m_1)^2, \end{aligned} \quad (5)$$

where G is the gravitational constant, P_1 is the orbital period of the first companion star, i_1 is the orbital inclination, m_1 is the mass of the first companion and $a_1' \sin i$ can be decided by,

$$a_1' \sin i_1 = c\sqrt{{a_1}^2 + {b_1}^2}. \quad (6)$$

The orbital parameters can then be computed from the Fourier coefficients (Kopal 1978) as follows

$$e_1 = 2\sqrt{\frac{{a_2}^2 + {b_2}^2}{{a_1}^2 + {b_1}^2}}, \quad (7)$$

Table 2 Parameters of the First Companion Star to CY Aqr

Parameter	Value	Unit
P_1	54.2	yr
e_1	0.49	
$a'_1 \sin i_1$	0.42	AU
$f(m_1)$	2.5462×10^{-5}	$M_\odot$
m_1 $(i_1 = 30°)$	0.09	$M_\odot$
m_1 $(i_1 = 60°)$	0.05	$M_\odot$
m_1 $(i_1 = 90°)$	0.04	$M_\odot$

Table 3 Parameters of the Second Companion Star to CY Aqr

Parameter	Value	Unit
P_2	47.3	yr
e_2	0.69	
$a'_2 \sin i_2$	0.21	AU
$f(m_2)$	4.349×10^{-6}	$M_\odot$
m_2 $(i_2 = 30°)$	0.05	$M_\odot$
m_2 $(i_2 = 60°)$	0.03	$M_\odot$
m_2 $(i_2 = 90°)$	0.02	$M_\odot$

where e_1 is the eccentricity of the long-period orbit for the first star and c is the speed of light. The orbital elements derived for the first star are listed in Table 2.

Using the same method, the orbital parameters of the second companion star can be obtained based on the following formulae:

$$\begin{aligned} f(m_2) &= 4\pi^2(a'_2 \sin i_2)^3/\mathrm{G}{P_2}^2 \\ &= (m_2 \sin i_2)^3/(M + m_2)^2, \end{aligned} \tag{8}$$

$$a'_2 \sin i_2 = c\sqrt{{c_1}^2 + {d_1}^2}, \tag{9}$$

$$e_2 = 2\sqrt{\frac{{c_2}^2 + {d_2}^2}{{c_1}^2 + {d_1}^2}}. \tag{10}$$

The orbital elements derived for the second star are listed in Table 3.

5 SUMMARY

According to the results above, the solution we used suggests that CY Aqr is very probably in a triple system orbited eccentrically by two low-mass companions. The orbital period of the first companion star is 54.2 yr and the eccentricity is 0.49. The orbital period of the second companion star is 47.3 yr and the eccentricity is 0.69. When the orbital inclination is 90°, the masses of the two companions are 0.04 $M_\odot$ and 0.02 $M_\odot$ respectively. The most plausible explanation is that the two companion stars are brown dwarfs. In order to verify the existence of the hidden companions, further photometric and spectroscopic observations are needed in the future.

Acknowledgements This work is supported by the National Natural Science Foundation of China (Nos. U1331121, 11373037 and U1231202).

References

Agerer, F., Dahm, M., & Hubscher, J. 1999, Information Bulletin on Variable Stars, 4712

Agerer, F., Dahm, M., & Hubscher, J. 2001, Information Bulletin on Variable Stars, 5017

Agerer, F., & Hubscher, J. 1996, Information Bulletin on Variable Stars, 4382

Agerer, F., & Hubscher, J. 2002, Information Bulletin on Variable Stars, 5296

Agerer, F., & Hubscher, J. 2003, Information Bulletin on Variable Stars, 5485

Agerer, F., & Huebscher, J. 1998a, Information Bulletin on Variable Stars, 4562

Agerer, F., & Huebscher, J. 1998b, Information Bulletin on Variable Stars, 4606

Ashbrook, J. 1949, AJ, 54, 168

Boonyarak, C., Fu, J.-N., Khokhuntod, P., & Jiang, S.-Y. 2011, Ap&SS, 333, 125

Braune, W., Huebscher, J., & Mundry, E. 1977, Astronomische Nachrichten, 298, 121

Braune, W., Huebscher, J., & Mundry, E. 1979, Astronomische Nachrichten, 300, 165
Chang, S.-W., Protopapas, P., Kim, D.-W., & Byun, Y.-I. 2013, AJ, 145, 132
Coates, D. W., Fernley, J. A., Sekiguchi, K., Barnes, T. G., & Frueh, M. L. 1994, MNRAS, 266, 1
Derekas, A., Kiss, L. L., Bedding, T. R., et al. 2009, MNRAS, 394, 995
Figer, A. 1978, Information Bulletin on Variable Stars, 1388
Fu, J. N., & Sterken, C. 2003, A&A, 405, 685
Hardie, R. H., & Tolbert, C. R. 1961, ApJ, 134, 581
Hubscher, J., Steinbach, H.-M., & Walter, F. 2009a, Information Bulletin on Variable Stars, 5889
Hubscher, J., Steinbach, H.-M., & Walter, F. 2009b, Information Bulletin on Variable Stars, 5874
Hubscher, J. 2011, Information Bulletin on Variable Stars, 5984
Hubscher, J., & Monninger, G. 2011, Information Bulletin on Variable Stars, 5959
Hubscher, J., & Lehmann, P. B. 2012, Information Bulletin on Variable Stars, 6026
Hubscher, J., Lehmann, P. B., & Walter, F. 2012, Information Bulletin on Variable Stars, 6010
Jensch, A. 1934, Astronomische Nachrichten, 253, 443
Kopal, Z., ed. 1978, Astrophysics and Space Science Library, 68, Dynamics of Close Binary Systems
Mahdy, H. A., & Szeidl, B. 1980, Commmunications of the Konkoly Observatory Hungary, 74, 1
Paschke, A. 2010, Open European Journal on Variable Stars, 130, 1
Percy, J. R. 1975, A&A, 43, 469
Powell, J. M., Joner, M. D., & McNamara, D. H. 1995, PASP, 107, 225
Rolland, A., Pena, J. H., Lopez de Coca, P., Peniche, R., & Gonzalez, S. F. 1986, A&A, 168, 125
Samolyk, G. 2014, Journal of the American Association of Variable Star Observers (JAAVSO), 42, 124
Samolyk, G. 2015, Journal of the American Association of Variable Star Observers (JAAVSO), 43, 74
Smak, J. 1959, Acta Astronomica, 9, 161
Sterken, C. 2005, in Astronomical Society of the Pacific Conference Series, 335, The Light-Time Effect in Astrophysics: Causes and Cures of the O-C Diagram, ed. C. Sterken, 3
Sterken, C., Wiedemair, C., Tuvikene, T., et al. 2011, Journal of Astronomical Data, 17
Sterken, C., Wiedemair, C., Munaro, T., et al. 2012, VizieR Online Data Catalog (other), 350
Tuvikene, T., Sterken, C., Brogt, E., et al. 2010, Journal of Astronomical Data, 16
Wils, P., Hambsch, F.-J., Robertson, C. W., et al. 2011, Information Bulletin on Variable Stars, 5977
Wils, P., Panagiotopoulos, K., van Wassenhove, J., et al. 2012, Information Bulletin on Variable Stars, 6015
Wils, P., Ayiomamitis, A., Vanleenhove, M., et al. 2013, Information Bulletin on Variable Stars, 6049
Wils, P., Ayiomamitis, A., Robertson, C. W., et al. 2014, Information Bulletin on Variable Stars, 6122
Yang, X. H., Fu, J. N., & Zha, Q. 2012, AJ, 144, 92